Clinical Cancer Research

Adrenergic Stimulation of DUSP1 Impairs Chemotherapy Response in Ovarian Cancer

Yu Kang[1,2], Archana S. Nagaraja[2], Guillermo N. Armaiz-Pena[2], Piotr L. Dorniak[2], Wei Hu[2], Rajesha Rupaimoole[2], Tao Liu[2], Kshipra M. Gharpure[2], Rebecca A. Previs[2], Jean M. Hansen[2], Cristian Rodriguez-Aguayo[3,4], Cristina Ivan[2,3], Prahlad Ram[5], Vasudha Sehgal[5], Gabriel Lopez-Berestein[3,4], Susan K. Lutgendorf[6], Steven W. Cole[7], and Anil K. Sood[2,3,8]

Abstract

Purpose: Chronic adrenergic activation has been shown to associate with adverse clinical outcomes in cancer patients, but the underlying mechanisms are not well understood. The focus of the current study was to determine the functional and biologic effects of adrenergic pathways on response to chemotherapy in the context of ovarian cancer.

Experimental Design: Increased DUSP1 production by sympathetic nervous system mediators (e.g., norepinephrine) was analyzed by real-time quantitative RT-PCR and by Western blotting. *In vitro* chemotherapy-induced cell apoptosis was examined by flow cytometry. For *in vivo* therapy, a well-characterized model of chronic stress was used.

Results: Catecholamines significantly inhibited paclitaxel- and cisplatin-induced apoptosis in ovarian cancer cells. Genomic analyses of cells treated with norepinephrine identified DUSP1 as a potential mediator. DUSP1 overexpression resulted in reduced paclitaxel-induced apoptosis in ovarian cancer cells compared with control; conversely, DUSP1 gene silencing resulted in increased apoptosis compared with control cells. DUSP1 gene silencing *in vivo* significantly enhanced response to paclitaxel and increased apoptosis. *In vitro* analyses indicated that norepinephrine-induced DUSP1 gene expression was mediated through ADRB2 activation of cAMP–PLC–PKC–CREB signaling, which inhibits JNK-mediated phosphorylation of c-Jun and protects ovarian cancer cells from apoptosis. Moreover, analysis of The Cancer Genome Atlas data showed that increased DUSP1 expression was associated with decreased overall ($P = 0.049$) and progression-free ($P = 0.0005$) survival.

Conclusions: These findings provide a new understanding of the mechanisms by which adrenergic pathways can impair response to chemotherapy and have implications for cancer management. *Clin Cancer Res; 22(7); 1713–24. ©2015 AACR.*

Introduction

Growing evidence points to adverse effects of chronic adrenergic stimulation on clinical outcomes in cancer patients (1). Stress and/or neuroendocrine stress hormones have been shown to reduce the efficacy of chemotherapy (2, 3). However, the molecular pathways involved in stress and impaired response to chemotherapy are not well known.

The effects of chronic stress on cancer growth and metastasis are potentially mediated by the sympathetic nervous system (SNS) and the hypothalamic–pituitary–adrenal (HPA) axis (4). Pretreatment with dexamethasone, an artificial glucocorticoid, has been shown to reduce the cytotoxic efficacy of chemotherapy (paclitaxel and doxorubicin) in breast cancer (5). In prostate cancer models, chronic sympathetic activation was found to reduce apoptotic signaling (6, 7). However, the effects of SNS mediators on chemotherapy response are not well understood. Here, we carried out a series of *in vitro* and *in vivo* studies to examine the functional and biologic effects of adrenergic pathways on response to chemotherapy in the context of ovarian cancer.

Materials and Methods

Drugs and reagents

The primary antibodies against ADRB1 and ADRB2 were purchased from Abcam. Anti-ADRB3 antibody, norepinephrine, isoproterenol, paclitaxel, α-adrenoceptor antagonist phentolamine, ADRA1 antagonist prazosin, ADRA2 antagonist yohimbine, ADRB1 antagonist atenolol, ADRB1 agonist dobutamine, ADRB2 antagonist ICI118,551, ADRB2 agonist terbutaline, ADRB3 antagonist SR59230A, MEK inhibitor U0126, PLC inhibitor U73122,

[1]Shanghai Key Laboratory of Female Reproductive Endocrine-Related Diseases, Obstetrics and Gynecology Hospital of Fudan University, Shanghai, P.R. China. [2]Department of Gynecologic Oncology and Reproductive Medicine, The University of Texas MD Anderson Cancer Center, Houston, Texas. [3]Center for RNAi and Non-Coding RNA, The University of Texas MD Anderson Cancer Center, Houston, Texas. [4]Department of Experimental Therapeutics, The University of Texas MD Anderson Cancer Center, Houston, Texas. [5]Systems Biology, The University of Texas MD Anderson Cancer Center, Houston, Texas. [6]Departments of Psychology, Obstetrics and Gynecology, and Urology and Holden Comprehensive Cancer Center, University of Iowa, Iowa City, Iowa. [7]Department of Medicine and Jonsson Comprehensive Cancer Center, University of California, Los Angeles School of Medicine, UCLA Molecular Biology Institute, and Norman Cousins Center, Los Angeles, California. [8]Cancer Biology, The University of Texas MD Anderson Cancer Center, Houston, Texas.

Note: Supplementary data for this article are available at Clinical Cancer Research Online (http://clincancerres.aacrjournals.org/).

Corresponding Author: Anil K. Sood, The University of Texas MD Anderson Cancer Center, 1155 Herman Pressler, Unit 1362, Houston, TX 77030. Phone: 713-745-5266; Fax: 713-792-7586; E-mail: asood@mdanderson.org

doi: 10.1158/1078-0432.CCR-15-1275

Translational Relevance

Mechanisms by which adrenergic pathways can reduce the efficacy of chemotherapy are not well understood. Here, we have found that norepinephrine-mediated increase in DUSP1 decreases the antitumor effects of commonly used chemotherapeutic agents. These findings provide a new understanding of how sustained adrenergic signaling leads to impaired chemotherapy response. Our data suggest that interventions targeting the sympathetic nervous system, such as β-blockers, could enhance the efficacy of chemotherapy in patients with ovarian and other cancers.

ADRB3-specific agonist BRL37344, cAMP agonist forskolin, PI3K inhibitor LY294002, AKT inhibitor AKT1/2, PKA inhibitor H-89, PKA inhibitor KT5720, and anti-β-actin (A5316) were purchased from Sigma-Aldrich. ADRB1 antagonist atenolol, nonspecific β-adrenergic antagonist propranolol and metoprolol, PKC inhibitor staurosporine, p38 inhibitor SB203580, Epac inhibitor brefeldin A, and Epac agonist 8CPT-2Me-cAMP were obtained from Tocris Bioscience. Anti-DUSP1 (MKP-1 and V-15) was acquired from Santa Cruz Biotechnology. Anti-cleaved caspase-3, anti-JNK, anti-pJNK, anti-c-Jun, anti-CREB, and anti-p-c-Jun were obtained from Cell Signaling Technology. Anti-Ki67 was acquired from Thermo Lab Vision. The following secondary antibodies were used for colorimetric immunohistochemical analysis: horseradish peroxidase-conjugated goat anti-rabbit immunoglobulin G (Jackson ImmunoResearch Laboratories) and the Vectastain ABC detection kit (Vector Laboratories). Docetaxel was purchased from Sanofi-Aventis. Recombinant Human vascular endothelial growth factor (VEGF) 165 was purchased from R&D Systems.

Cell lines and culture conditions

Ovarian cancer cell lines (SKOV3ip1, SKOV3-TR, HeyA8, HeyA8-MDR, A2780, A2780-CP20, IGROV-1, ES2, OVCAR3, and OVCAR5), an ovarian epithelial cell line (HIO-180), and a breast cancer cell line (MDA-231) were cultured as previously described (4). In brief, all cell lines were maintained in RPMI-1640 medium that was supplemented with 10% fetal bovine serum and 0.1% gentamicin sulfate (Gemini BioProducts) in 5% CO_2 and 95% air at 37°C. Cells were routinely screened for mycoplasma species (GenProbe detection kit; Fisher Scientific). All experiments were performed with 70% to 80% confluent cultures.

Real-time quantitative RT-PCR analysis

Quantitative RT-PCR was performed to assess DUSP1 mRNA expression in ovarian cancer cells (HeyA8 and SKOV3ip1) after the cells were treated with increasing doses of norepinephrine and isoproterenol using the RNAqueous kit (Ambion), following the manufacturer's protocols. For blocking experiments, cells were pretreated with propranolol (10 μm) or specific antagonist (10 μmol/L) for 3 hours prior to treatment with norepinephrine or isoproterenol. Cells were then washed twice with phosphate-buffered saline (PBS) and kept at −80°C for at least 20 minutes. The mirVana kit (Ambion) was used for RNA extraction according to the manufacturer's guidelines. The mRNA was then transcribed into cDNA using Verso cDNA synthesis kit (Thermo Scientific). Quantitative RT-PCR was performed in the Applied Biosystems 7500 series using conditions that have been previously described (8), using SYBR Green Master Mix (Applied Biosystems) in triplicate. β-Actin was used as an endogenous control. Mean fold change was reported.

In vitro gene silencing

Human DUSP1 siRNA 1 (Cat. No. SASI_Hs01_00098747) and human DUSP1 siRNA2 (Cat. No. SASI_Hs02_00337565) were purchased from Sigma-Aldrich and used to silence DUSP1 expression in ovarian cancer cell lines. A nonsilencing siRNA that did not share sequence homology with any known human mRNA, according to a BLAST search, was used as a control for target siRNA. In brief, SKOV3ip1 and HeyA8 ovarian cancer cells were reverse transfected with siRNA (20 nmol/L) using Lipofectamine RNAiMAX transfection reagent (Invitrogen Corp), according to the manufacturer's instructions. After being transfected for 48 hours, the cells were serum starved for 6 hours and untreated or treated with paclitaxel for 72 hours. Cells were collected as lysates. DUSP1 expression was determined by Western blot analysis.

Apoptosis assay

Apoptosis was carried out using annexin V phycoerythrin/7AAD staining (BD Biosciences) with flow cytometry, as previously described (9). In brief, 72 hours after treatment with paclitaxel, ovarian cancer cells were washed twice with cold PBS and resuspended in 1× binding buffer at a concentration of 1×10^6 cells/mL. Cells (1×10^5) were then incubated with 5 μL of annexin V phycoerythrin and 5 μL of 7AAD. Cells were gently vortexed and then incubated for 15 minutes at ambient temperature (25°C) in the dark. After the addition of 400 μL of 1× binding buffer, samples were analyzed using flow cytometry.

Western blot analysis

Lysates from cultured cells were prepared as previously described (9). In brief, cells at 80% confluence were harvested and lysed in modified radioimmunoprecipitation assay buffer (50 mmol/L Tris, 150 mmol/L NaCl, 1% Triton X-100, 0.5% deoxycholate, 25 μg/mL leupeptin, 10 μg/mL aprotinin, 2 mmol/L EDTA, and 1 mmol/L sodium orthovanadate). Cells were removed by scraping and centrifuged at 8,000× *g* rotations per minute for 10 minutes. The protein concentration of the supernatant was determined using a bicinchoninic acid protein assay reagent kit (Pierce Chemical). Typically, 30 μg of protein was fractionated by 10% SDS-PAGE, transferred to a nitrocellulose membrane (Bio-Rad Laboratories), blocked with 5% nonfat milk in TBS-T [10 mmol/L Tris (pH 8), 150 mmol/L NaCl, and 0.05% Tween-20] for 1 hour at ambient temperature, and incubated with primary antibodies at 4°C overnight. Antibodies were detected using 0.167 μg/mL horseradish peroxidase–conjugated secondary antibody (The Jackson Laboratory) and developed using an enhanced chemiluminescence detection kit (Pierce Chemical). A densitometric analysis was performed using ImageJ software (NIH) to interpret the differences in Western blot results, using total DUSP1, JNK, c-Jun, or β-actin as a control for each sample.

Orthotopic mouse model of chronic stress

For the chronic stress model, we used a physical restraint system that had been previously used by our research group (4). Female athymic nude mice (8–12 weeks old) were purchased from the NCI–Frederick Cancer Research and Development Center (Frederick, MD) and housed in pathogen-free conditions in an animal

facility that is approved by the American Association for Accreditation of Laboratory Animal Care, in agreement with the current regulations and standards of the United States Department of Agriculture, Department of Health and Human Services, and the National Institutes of Health. The study protocols were approved and supervised by the Institutional Animal Care and Use Committee at MD Anderson. In brief, mice were subjected to daily restraint stress for 7 days prior to tumor cell inoculation; this stress continued until the end of the experiment. Mice were killed and necropsied on day 35 (SKOV3ip1) or day 28 (HeyA8) after tumor cell injection. The tumors were harvested for immunohistochemical analysis and weighed, and the number of tumor nodules was recorded.

In vivo therapeutic experiments

Human ovarian cancer cells (SKOV3ip1 and HeyA8) were grown in culture, collected (SKOV3ip1 and trypsin in EDTA or HeyA8 in EDTA), and centrifuged at 1,000 rotations per minute for 7 minutes at 4°C. Cells were then washed with Hanks' balanced salt solution (HBSS; Invitrogen). Only single-cell suspensions with >95% viability, as determined by trypan blue exclusion, were used for the *in vivo* injections. To produce tumors, we injected SKOV3ip1 cells (1×10^6 cells per 0.2 mL of HBSS; Life Technologies and Invitrogen) or HeyA8 cells (2.5×10^5 cells per 0.2 mL of HBSS) into the peritoneal cavities of the mice. Mice were monitored daily for adverse effects of therapy and were killed on day 35 (SKOV3ip1), day 28 (HeyA8), or when any of the mice seemed moribund. The total body weight, tumor incidence and mass, and number of tumor nodules were recorded. Tumors were fixed in formalin and embedded in paraffin or snap frozen in optimal cutting temperature compound (Sakura Finetek USA, Inc.) in liquid nitrogen.

To determine the effects of stress on chemotherapy, we injected SKOV3ip1 or HeyA8 cells into the peritoneal cavity of mice. One week after tumor cell injection, mice were randomly assigned to 1 of 8 groups (10 mice each), 4 without stress and 4 with stress treated with control, paclitaxel alone, propranolol alone, or paclitaxel with propranolol. Treatment was initiated 3 to 4 weeks after injection. Paclitaxel (2 mg/kg for SKOV3ip1 cells or 2.5 mg/kg for HeyA8 cells) was administered intraperitoneally weekly; propranolol (2 mg/kg) was administered intraperitoneally every day. Control mice received HBSS intraperitoneally.

To evaluate the role of DUSP1 in stress-induced chemoresistance, we subjected mice to daily restraint stress 1 week after cell injection. Seven days later, mice were randomly assigned to 1 of 4 groups ($n = 10$ mice per group): (i) control siRNA, (ii) control siRNA and paclitaxel, (iii) DUSP1 siRNA, or (iv) DUSP1 siRNA and paclitaxel. Targeted siRNA (5 μg/mouse) was administered twice weekly until the end of the experiment.

Immunohistochemical analysis

Immunohistochemical analysis was prepared as previously described (9). Antigen retrieval was performed using a Borg Decloaker (BioCare Medical) that included a pressure cooker for cleaved caspase-3, citrate buffer (0.1 mol/L, pH 6.0) with a steamer for anti-DUSP1 and anti-pJNK, Diva (BioCare Medical) with a steamer for anti-Ki67, and pepsin in a 37°C humidified incubator for vascular endothelial growth factor. Endogenous peroxidase and nonspecific epitopes were blocked with 3% H_2O_2 (Fisher Scientific) in PBS for 12 minutes at ambient temperature; nonspecific protein binding was blocked with 5% normal horse serum and 1% normal goat serum for anti-Ki67 antibody or with 4% fish skin gelatin (Electron Microscopy Science) for 20 minutes at ambient temperature for anti-cleaved caspase-3 and anti-DUSP1.

Sections were incubated with primary antibodies in blocking solution overnight at 4°C at the following dilutions: anti-DUSP1, 1:100; anti-pJNK, 1:100; anti-Ki67, 1:500; and anti-cleaved caspase-3, 1:1,000. For the negative control, sections were incubated without primary antibody and with human immunoglobulin G antibody. After sections were washed with PBS, followed by Optimax buffer, the appropriate secondary antibody was applied, and visualization was performed using the Vectastain ABC detection kit, according to the manufacturer's instructions. Goat anti-rabbit horseradish peroxidase–conjugated antibodies for anti-DUSP1, anti-Ki67, and anti-cleaved caspase-3 (1 hour, ambient temperature) were used for secondary antibodies. The chromogenic reaction was performed with 3,3′-diaminobenzidine (Phoenix Biotechnologies), and counterstaining was performed using Gill's no. 3 hematoxylin (Sigma-Aldrich). To quantify Ki67 and cleaved caspase-3 expression, we counted the number of positive tumor cells in 10 random fields at ×200 magnification. For DUSP1 and p-JNK levels, the slides were stained with respective antibodies and staining intensity assessed semi-quantitatively. In short, 5 random fields were chosen per slide and scored from 0 to 4 on intensity and 0% to 100% on distribution of positive staining of tumor tissue. The final results per group are presented in the accompanying graph with representative pictures for each group.

DUSP1 promoter analysis

HeyA8 (3×10^5) cells were transfected (Lipofectamine 2000; Invitrogen) with a dual luciferase reporter construct (SwitchGear Genomics) in which Firefly luciferase gene transcription was driven by a human *DUSP1* promoter sequence spanning 914 base pairs (bp) upstream of the RefSeq transcription start site. Cells were treated with vehicle control solutions, 1 or 10 μmol/L norepinephrine, or indicated adrenergic agonists and antagonists (all from Sigma) and harvested 3 to 4 hours later for dual luciferase assay (Promega). To localize norepinephrine-responsive elements, we compared induction of the full-length (−914) *DUSP1* promoter sequence with that of successively truncated variants (100-bp decrements for gross localization, followed by 20-bp decrements for fine localization; GeneWiz). Within the identified norepinephrine-responsive region, potential transcription factor–binding sites were identified through standard position-specific weight matrix scans (TRANSFAC and Jaspar motif libraries). Functional activity of putative binding sites was assessed using site-directed mutagenesis (GeneWiz) to abrogate core binding sequences. Transcription factor activation in response to norepinephrine was assessed by enzyme-linked immunosorbent assay (Signosis) of 5 μg of nuclear protein (CelLytic NuCLEAR; Sigma) harvested after 5 minutes or 20 minutes of exposure to vehicle control or 10 μmol/L norepinephrine. All data represent the average of 5 independent studies.

The Cancer Genome Atlas (TCGA)

Affymetrix level 2 mRNA, Agilent level 2 microRNA and RNA-Seq level 3 data for patients with HGS-OvCa were downloaded from the public TCGA data portal.

Statistical analysis

All results are expressed as the mean ± SEM. Continuous variables were compared using the Student *t* test or analysis of variance. Statistical analyses were performed using Statistical Package for Social Science software (SPSS, version 18.0). Only two-tailed values are reported. We considered $P < 0.05$ to be statistically significant for survival analysis the patients were grouped into percentiles according to DUSP1 expression. The log-rank test was employed to determine the association between mRNA expression and survival and the Kaplan–Meyer method was used to generate survival curves. Cutoff points to significantly split (log-rank test $P < 0.05$) the samples into low/high DUSP1 groups were recorded. Survival analyses were performed using Cox regression analysis.

Results

Catecholamines inhibit chemotherapy-induced apoptosis

Given the sustained increase in catecholamine levels under chronic stress settings, we first examined potential effects on apoptotic response to chemotherapy. We analyzed the effects of norepinephrine on the efficacy of paclitaxel and cisplatin (first-line treatment for advanced ovarian cancer) in two ovarian cancer cell lines (HeyA8 and SKOV3ip1). In HeyA8 cells, pretreatment with norepinephrine prior to treatment with paclitaxel resulted in significantly reduced apoptosis compared to paclitaxel alone ($P = 0.003$; Fig. 1A). Similarly, in HeyA8 cells treated with cisplatin, cells pretreated with norepinephrine had a 53.1% lower apoptosis rate than cells treated with cisplatin alone ($P = 0.01$; Fig. 1B). We also tested the effects of the synthetic β-agonist isoproterenol and found that this caused a similar reduction in the efficacy of both paclitaxel (Fig. 1A) and cisplatin (Fig. 1B). We next pretreated ovarian cancer cells with the nonselective β-blocker propranolol for 30 minutes prior to norepinephrine or isoproterenol exposure. As shown in Fig. 1A, propranolol treatment completely abrogated the effects of norepinephrine in HeyA8 ovarian cancer cells. Similar effects were observed with the SKOV3ip1 cells ($P < 0.05$; Fig. 1C and D).

Catecholamines increase DUSP1 production

To identify the mechanisms underlying the effects of catecholamines on response to chemotherapy, we performed genomic

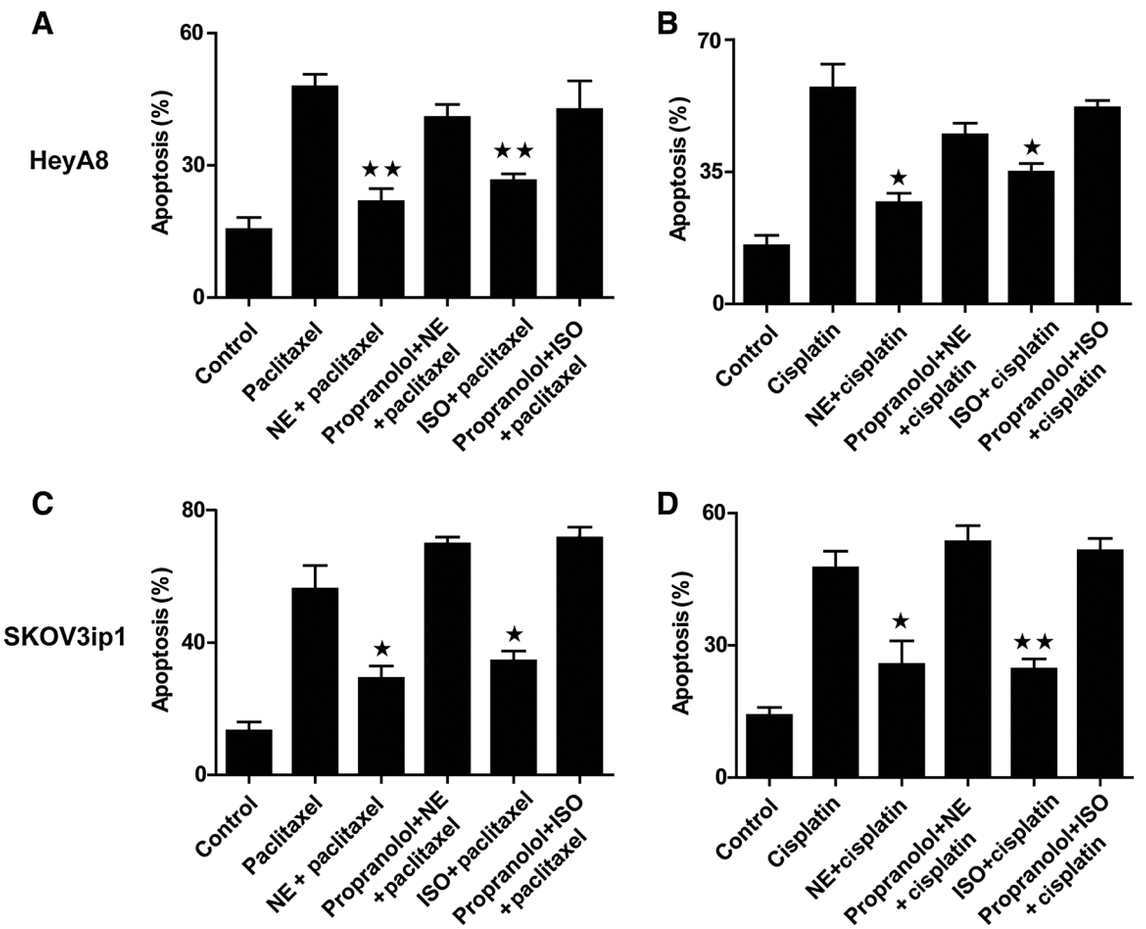

Figure 1.

Catecholamines inhibit chemotherapy-induced apoptosis in ovarian cancer cells. HeyA8 (A and B) and SKOV3ip1 (C and D) cells were treated with the chemotherapeutic agents paclitaxel (A and C) or cisplatin (B and D), alone (IC_{50}) or in combination with the catecholamines norepinephrine (NE; 10 μmol/L) or isoproterenol (ISO; 10 μmol/L). A β-blocker (propranolol; 1 μmol/L) was administered 30 minutes prior to catecholamine exposure. Apoptosis assays were performed using annexin V phycoerythrin/7AAD, followed by flow cytometry analysis. Results shown represent mean ± SEM, indicated by the error bar. *, $P < 0.05$; **, $P < 0.01$, compared with paclitaxel or cisplatin alone.

analyses of HeyA8 and SKOV3ip1 ovarian cancer cells following exposure to norepinephrine (10). These analyses showed that the MAPK phosphatase DUSP1 and its downstream network were significantly altered in both cell lines, compared with control cells (Supplementary Fig. S1A and S1B). We found that DUSP1 expression was significantly higher in cells treated with norepinephrine than in control cells (Fig. 2A). To validate these findings, we stimulated ovarian cancer cells with increasing concentrations of norepinephrine or isoproterenol in independent experiments. DUSP1 levels were assessed by qRT-PCR after 1, 3, or 6 hours of exposure to norepinephrine or isoproterenol (Fig. 2B), followed by Western blot analysis (Fig. 2C). There were significant increases in DUSP1 mRNA levels following norepinephrine or isoproterenol treatment. Propranolol completely abrogated the effects of norepinephrine on DUSP1 induction (Fig. 2C).

ADRB2 is a key mediator of increased DUSP1 levels

To determine whether DUSP1 expression is regulated through β-adrenergic receptors, we first screened ADRB1, ADRB2, ADRB3, and DUSP1 expression in 10 epithelial ovarian cancer cell lines and one breast cancer cell line (MDA-231), using nontransformed ovarian surface epithelial HIO-180 cells as control. Supplementary Fig. S2A shows the baseline expression of β-adrenergic receptors and DUSP1 in these cells. A2780 cells were negative for ADRB1, ADRB2, and with very weak expression of ADRB3. DUSP1 mRNA levels were assessed 3 hours after exposure to 10 μmol/L norepinephrine. As shown in Supplementary Fig. S2B, in ADRB2-positive cancer cells, treatment with norepinephrine resulted in significantly higher DUSP1 mRNA levels compared with control ($P < 0.01$), whereas in ADRB2-negative cancer cells, norepinephrine had no significant effect on DUSP1 levels.

To determine whether α-adrenergic receptors were involved in increasing levels of DUSP1 or not, we treated HeyA8 cells with α-adrenergic receptor antagonists (ADRA1 antagonist prazosin and ADRA2 antagonist yohimbine; Fig. 2D) and found that there was no effect on norepinephrine-induced DUSP1 expression. We then found that inhibition with propranolol abrogated norepinephrine-induced DUSP1 expression in ovarian cancer cells (Fig. 2E). We also tested more specific ADRB blockers; atenolol (ADRB1 antagonist) had little effect on norepinephrine-induced DUSP1 expression, but 1 μmol/L and 10 μmol/L ICI118,551 (ADRB2 antagonist) and SR59230A (ADRB3 antagonist) markedly decreased norepinephrine-induced increases in DUSP1 expression ($P < 0.01$; Fig. 2F). Furthermore, using ADRB2 and ADRB3 siRNAs, we found that norepinephrine-induced DUSP1 expression occurs predominantly through ADRB2 ($P < 0.01$; Fig. 2G).

Norepinephrine-mediated transcriptional regulation of DUSP1 promoter

To further delineate the mechanism of norepinephrine-mediated DUSP1 expression, we examined the effects of norepinephrine (3 hours) on a *DUSP1* luciferase promoter construct in HeyA8 ovarian cancer cells (Fig. 3A). Treatment with norepinephrine resulted in ∼3-fold increase in *DUSP1* promoter activity compared with control ($P < 0.05$). However, pretreatment of cells with an ADRB2-selective antagonist (ICI118,551) efficiently blocked the effects of norepinephrine. Antagonists of ADRB1 and ADRB3 receptors (metoprolol and SR59230A) had no effect. We also tested the effects of specific β-agonists (the ADRB1-selective agonist dobutamine, the ADRB2-selective agonist terbutaline, or the ADRB3-selective agonist BRL37344); both nonselective β-adrenergic stimulation (isoproterenol) and selective activation of ADRB2 proved sufficient to stimulate *DUSP1* promoter activity to levels commensurate with the effects of norepinephrine.

To identify the specific transcription factor and promoter response element mediating norepinephrine induction of the *DUSP1* promoter, we conducted systematic mutagenesis of a luciferase reporter construct under control of the 914 bp DNA sequence upstream of the human *DUSP1* transcription start site (Fig. 3B–E). A series of 100-bp and subsequent 20-bp deletion constructs localized the norepinephrine responsive region of the *DUSP1* promoter to a region ranging between −174 and −154 bp upstream of the transcription start site ($P < 0.05$; Fig. 3B and C). Bioinformatic analysis of this sequence identified multiple transcription factor–binding motifs (Fig. 3D), including potential response elements for Sp1, NF1, AP-2, MZF (Myeloid Zinc Finger proteins), and Ets family transcription factors. Systematic abrogation of target binding sites for each factor further localized the norepinephrine-responsive region of the *DUSP1* promoter to a CCC repeat spanning −162 to −165 bp ($P < 0.05$; Fig. 3E). Among the transcription factors predicted to bind to this region, only Sp1 showed significant activation by norepinephrine (1.9-fold ± 0.4-fold, $P = 0.03$; Fig. 3F).

To further elucidate the role of ADRB2 in norepinephrine-mediated DUSP1 induction, we inhibited several downstream proteins in the ADRB2 pathway. Because cAMP is an important component of the ADRB2 signaling pathway, we tested the effects of forskolin (cAMP activator) on DUSP1 gene expression. DUSP1 levels were significantly increased in response to forskolin (Fig. 4A). Downstream of cAMP are several proteins, including PLC, PKA, and Epac. The PLC inhibitor U73122 markedly decreased norepinephrine-induced increases in DUSP1 expression in SKOV3ip1 cells (Fig. 4B). Inhibition of factors downstream of PLC suggested the involvement of PKC (inhibitor staurosporine; Fig. 4B). We then examined DUSP1 expression following treatment with siRNA targeted against PKC, CREB1, or SP1, respectively. As shown in Fig. 4C, after PKC, CREB1 and SP1 downregulation, norepinephrine-induced DUSP1 expression was significantly decreased. Meantime, inhibition of additional downstream proteins, including PI3K (inhibitor LY294002; Fig. 4D), Akt (Akt1/2 kinase inhibitor; Fig. 4D), Epac (inhibitor brefeldin A and activator 8CPT-2Me-cAMP; Fig. 4E), PKA (inhibitor KT5720 and H-89; Fig. 4F), MEK (inhibitor U0126; Fig. 4G), and p38 (inhibitor SB203580; Fig. 4H), had no significant effect on norepinephrine-induced DUSP1 expression. Similar results were observed for HeyA8 cells (data not shown).

Blocking DUSP1 inhibits norepinephrine-induced dephosphorylation of JNK and c-Jun

Some studies have suggested that DUSP1, as a MAPK phosphatase, is an important regulator of JNK-dependent apoptosis. For example, DUSP1 overexpression can inhibit JNK-mediated phosphorylation of c-Jun and protect sympathetic neurons from apoptosis (11). To determine whether norepinephrine activates JNK and c-Jun, we treated HeyA8 cells with or without norepinephrine (10 μmol/L) for various time periods prior to treatment with paclitaxel. The baseline expression of p-JNK and p-c-Jun (0-hour time point) was weak and expression of p-JNK and p-c-Jun increased at a peak of 6 hours after treatment with paclitaxel; however, JNK and c-Jun phosphorylation was inhibited as a result of pretreatment with norepinephrine (Fig. 4I).

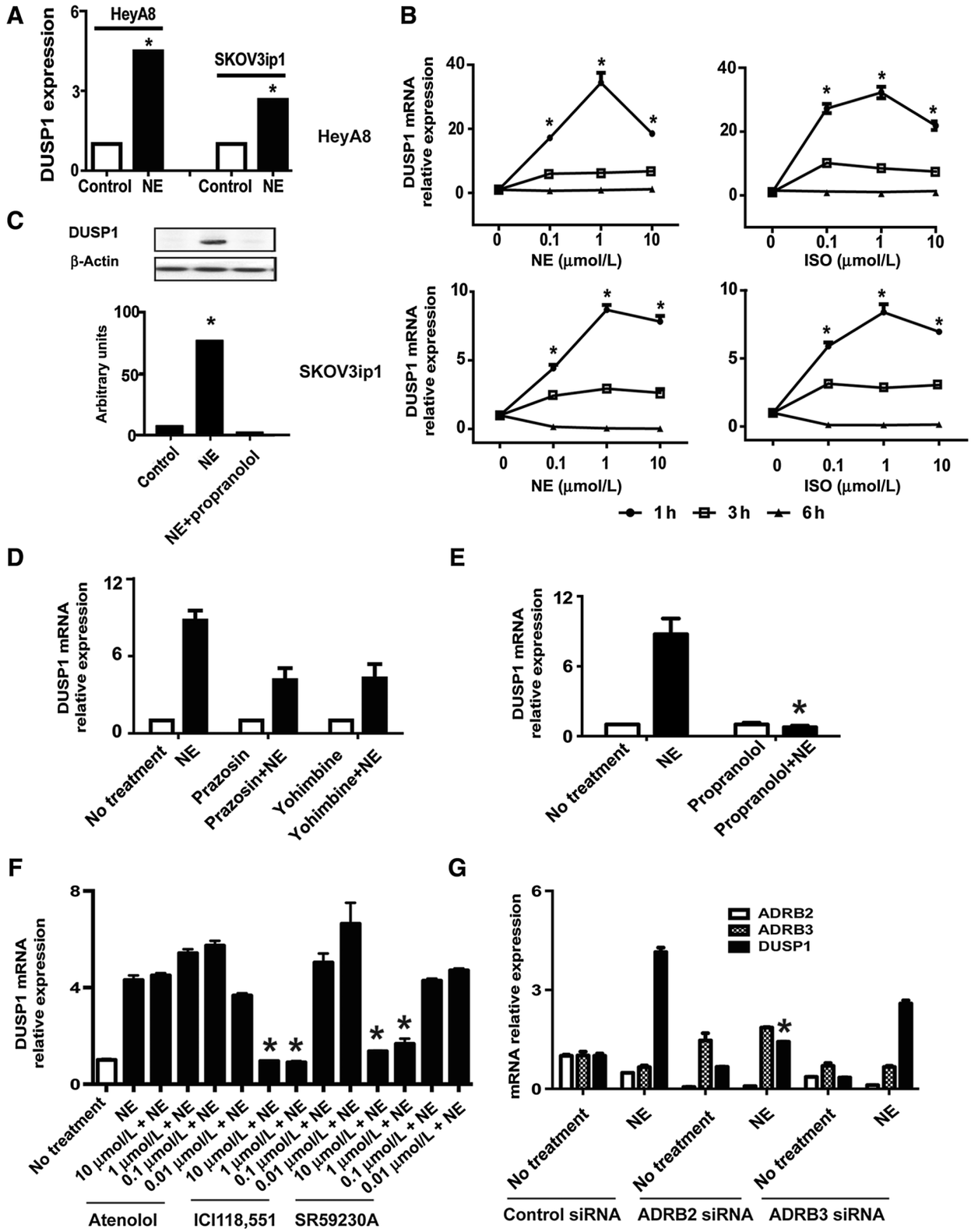

Figure 2.

Catecholamines increase DUSP1 production through ADRB2. A, DUSP1 gene expression in HeyA8 and SKOV3ip1 ovarian cancer cells treated with norepinephrine (NE) compared with untreated cells (*, $P < 0.01$). B, DUSP1 mRNA levels, determined by real-time RT-PCR in HeyA8 and SKOV3ip1 ovarian cancer cells after exposure to different concentrations (0, 0.1, 1, or 10 μmol/L) of norepinephrine or isoproterenol (ISO) for different time periods (1, 3, or 6 hours). (*Continued on the following page.*)

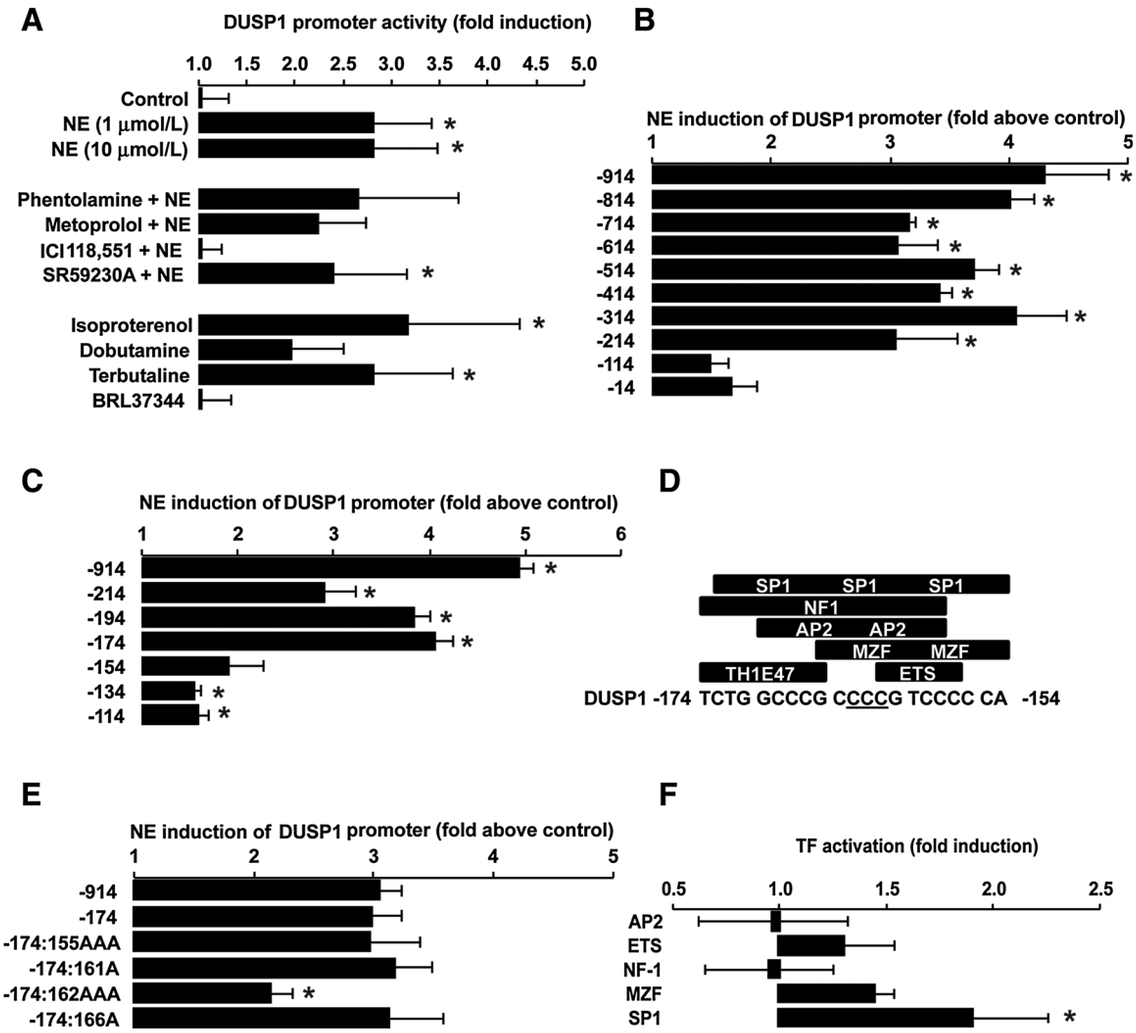

Figure 3.

Norepinephrine (NE) plays a role in transcriptional control of DUSP1 promoter. A, DUSP1 promoter activity was determined by expression of a luciferase reporter gene in HeyA8 ovarian cancer cells after 3 hours of exposure to norepinephrine (1 or 10 μmol/L) or an equivalent volume of vehicle control solution. The role of specific β-adrenergic receptors in mediating norepinephrine effects on DUSP1 promoter activity was assessed by pretreating cells for 2 hours with 1 μmol/L concentrations of the α-adrenergic antagonist phentolamine, the ADRB1-selective antagonist metoprolol, the ADRB2-selective antagonist ICI118,551, or the ADRB3-selective antagonist SR59230A. To determine whether β-adrenergic signaling alone was sufficient to activate the DUSP1 promoter, cells were treated with 1 μmol/L concentrations of the nonselective β-agonist isoproterenol, the ADRB1-selective agonist dobutamine, the ADRB2-selective agonist terbutaline, or the ADRB3-selective agonist BRL37344. Values, mean ± standard error of 5 independent experiments. *, $P < 0.05$, compared with vehicle-treated control condition. B–E, to identify the specific transcription factor and promoter response element mediating norepinephrine induction of the DUSP1 promoter, we conducted systematic mutagenesis of a luciferase reporter construct under control of the 914 bases upstream of the human DUSP1 transcription start site. B and C, *, $P < 0.05$, compared with vehicle-treated control condition; E, *, $P < 0.05$, compared with the full-length promoter construct in the magnitude of norepinephrine-induced luciferase activity. F, transcription factors activated by norepinephrine. *, $P < 0.05$, compared with vehicle-treated control condition.

To determine whether DUSP1 induction is required for norepinephrine-mediated dephosphorylation of JNK and c-Jun, we examined JNK and c-Jun phosphorylation along with DUSP1 siRNA (Supplementary Fig. S3A). As shown in Fig. 4J, DUSP1 siRNA-expressing cells retained JNK and c-Jun phosphorylation after 24 hours of treatment with norepinephrine

(*Continued.*) The mean fold change in DUSP1 mRNA expression compared with control is shown. Error bars, SEM. *, $P < 0.01$, compared with vehicle-treated control condition. C, Western blots analysis of DUSP1 protein expression. HeyA8 cells were stimulated with 10 μmol/L norepinephrine for 3 hours, and protein was obtained from the cell lysate for Western blot analysis using a DUSP1 antibody. The quantification of band intensity relative to β-actin intensity is shown at the bottom. *, $P < 0.01$, compared with the control. Adrenergic signaling plays a role in DUSP1 production. HeyA8 cells were pretreated with receptor-specific agonists or inhibitors and stimulated with norepinephrine for 3 hours; DUSP1 mRNA expression levels were then examined using real-time RT-PCR. Data, percentage of the control (medium only). The relative DUSP1 mRNA level is graphed as the mean fold change in DUSP1 production relative to control. Error bars, SEM. D, ADRA1 antagonist prazosin and ADRA2 antagonist yohimbine. E, nonspecific β-adrenergic antagonist propranolol. *, $P < 0.01$, compared with the norepinephrine-treated only. F, ADRB1 antagonist atenolol, ADRB2 antagonist ICI118,551, and ADRB3 antagonist SR59230A. *, $P < 0.01$, compared with the norepinephrine-treated only. G, ADRB2 and ADRB3 siRNA. *, $P < 0.01$, compared with control siRNA.

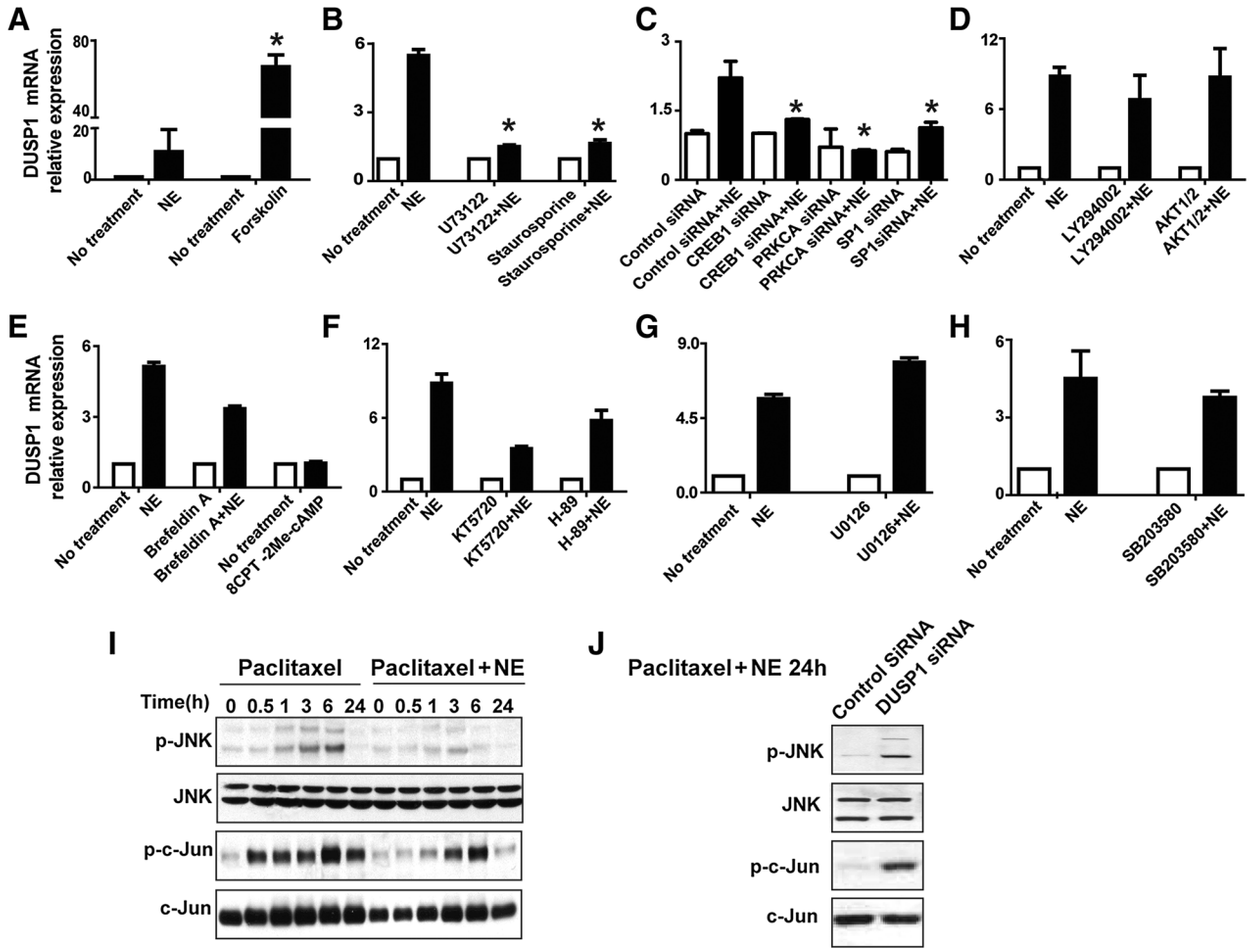

Figure 4.

Downstream signaling of ADRB2 is involved in norepinephrine(NE)-induced increases in DUSP1 expression. A, cAMP agonist forskolin. B, PLC inhibitor U73122 and PKC inhibitor staurosporine. C, PKC, CREB1, and SP1 siRNA. D, PI3K inhibitor LY294002 and AKT inhibitor AKT1/2. E, Epac inhibitor brefeldin A and Epac agonist 8CPT-2Me-cAMP. F, PKA inhibitor KT5720 and H-89. G, MEK inhibitor U0126. H, p38 inhibitor SB203580. Error bars, SEM. DUSP1 siRNA inhibits norepinephrine-induced dephosphorylation of JNK and c-Jun. I, Western blot analysis of p-JNK (p-JNK1 and p-JNK2) and p-c-Jun, evaluated using the appropriate phospho-specific antibodies. Total JNK and total c-Jun are shown for comparison. These results represent 3 independent experiments. J, Western blot analysis of JNK/c-Jun phosphorylation after 24 hours of treatment with norepinephrine and paclitaxel in DUSP1 siRNA-expressing cells.

and paclitaxel, and control siRNA-expressing cells showed the characteristic norepinephrine-mediated inhibition of JNK and c-Jun phosphorylation. These data suggest that DUSP1 inhibition, which augmented apoptosis, resulted in enhanced p-JNK and p-c-Jun levels.

Chronic restraint stress reduces the efficacy of chemotherapy *in vivo*

We examined the effects of adrenergic activation *in vivo* on response to chemotherapy using a well-characterized model of chronic stress (4). In this model, daily restraint stress was associated with a 330% higher mean tumor weight in HeyA8 tumors ($P = 0.019$; Fig. 5A, left) and a 296% higher mean tumor weight in SKOV3ip1 tumors ($P = 0.0005$; Fig. 5B, left) compared with control (no stress). Daily restraint stress also led to a higher mean number of tumor nodules (278% increase in HeyA8 cells, $P = 0.0112$, Fig. 5A, right; and 302% increase in SKOV3ip1 cells, $P = 0.0067$, Fig. 5B, right). Moreover, daily restraint stress decreased the efficacy of docetaxel chemotherapy (Fig. 5A and B). The addition of propranolol enhanced the effects of docetaxel even under daily restraint stress.

Next, we examined the biologic effects (i.e., effects on cell apoptosis and proliferation of daily restraint stress in the samples obtained from the *in vivo* experiments. While daily restraint stress was associated with reduced docetaxel-induced apoptosis $P < 0.0001$, the addition of propranolol restored the effects of chemotherapy ($P = 0.0167$; Fig. 5C). The effects on proliferation were more modest ($P = 0.0242$; Fig. 5D).

We also examined DUSP1 and JNK phosphorylation in these samples. The DUSP1 expression was substantially higher in the stress group compared with controls (Fig. 5E) and inhibition with propranolol abrogated stress-induced DUSP1 expression (Fig. 5E). The expression of p-JNK was decreased in the stress group (Fig. 5F) and increased in the docetaxel group (Fig. 5F). Propranolol treatment resulted in increased p-JNK levels in the stress group (Fig. 5F).

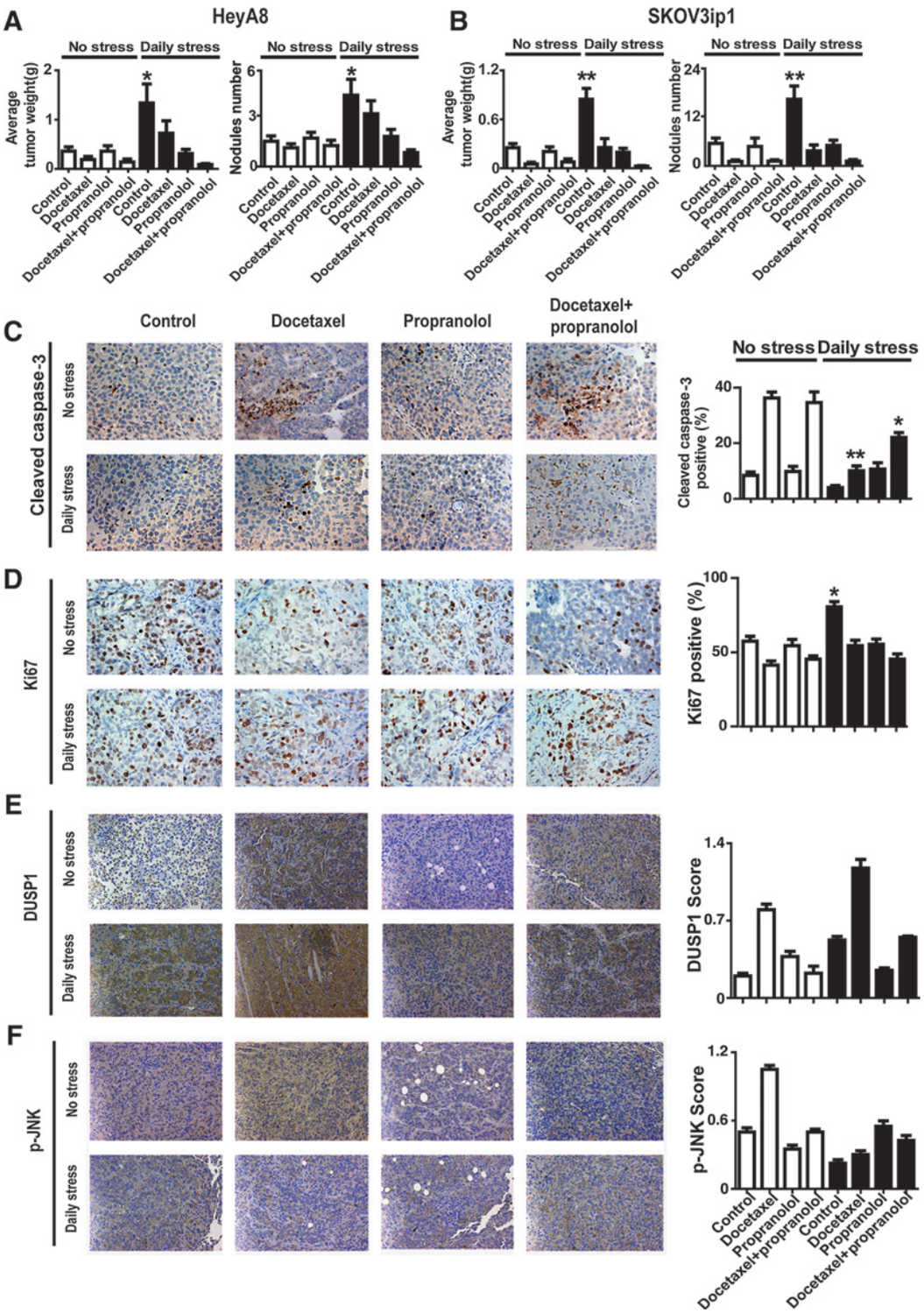

Figure 5.
Effects of chronic restraint stress on ovarian cancer chemosensitivity. One week after being intraperitoneally injected with HeyA8 (A) or SKOV3ip1 (B) cells, nude mice were subjected to 2 hours of daily restraint stress each morning until the end of the experiment. Mice were randomly assigned to 8 groups (10 mice each, 4 without stress and 4 with stress treated with control, paclitaxel alone, propranolol alone, or paclitaxel with propranolol). Treatment was initiated at 3 to 4 weeks after injection. Paclitaxel at a dose of 2 mg/kg (SKOV3ip1) or 2.5 mg/kg (HeyA8) was given intraperitoneally weekly; propranolol at a dose of 2 mg/kg was given intraperitoneally every day. At the end of the study, mice were killed and their tumors were harvested. Tumor weights (A and B, left) and tumor nodules (A and B, right) were quantified in the HeyA8 and SKOV3ip1 models. Immunohistochemical staining of tumor samples from the SKOV3ip1 model showing the effects of chronic restraint stress on cell apoptosis (C), proliferation (D), DUSP1 (E), and JNK phosphorylation (F). All photographs were taken at 200× magnification. The bars in the graphs correspond sequentially to the labeled columns of the images at left. Error bars, SEM. *, $P < 0.05$; **, $P < 0.01$, compared with the control.

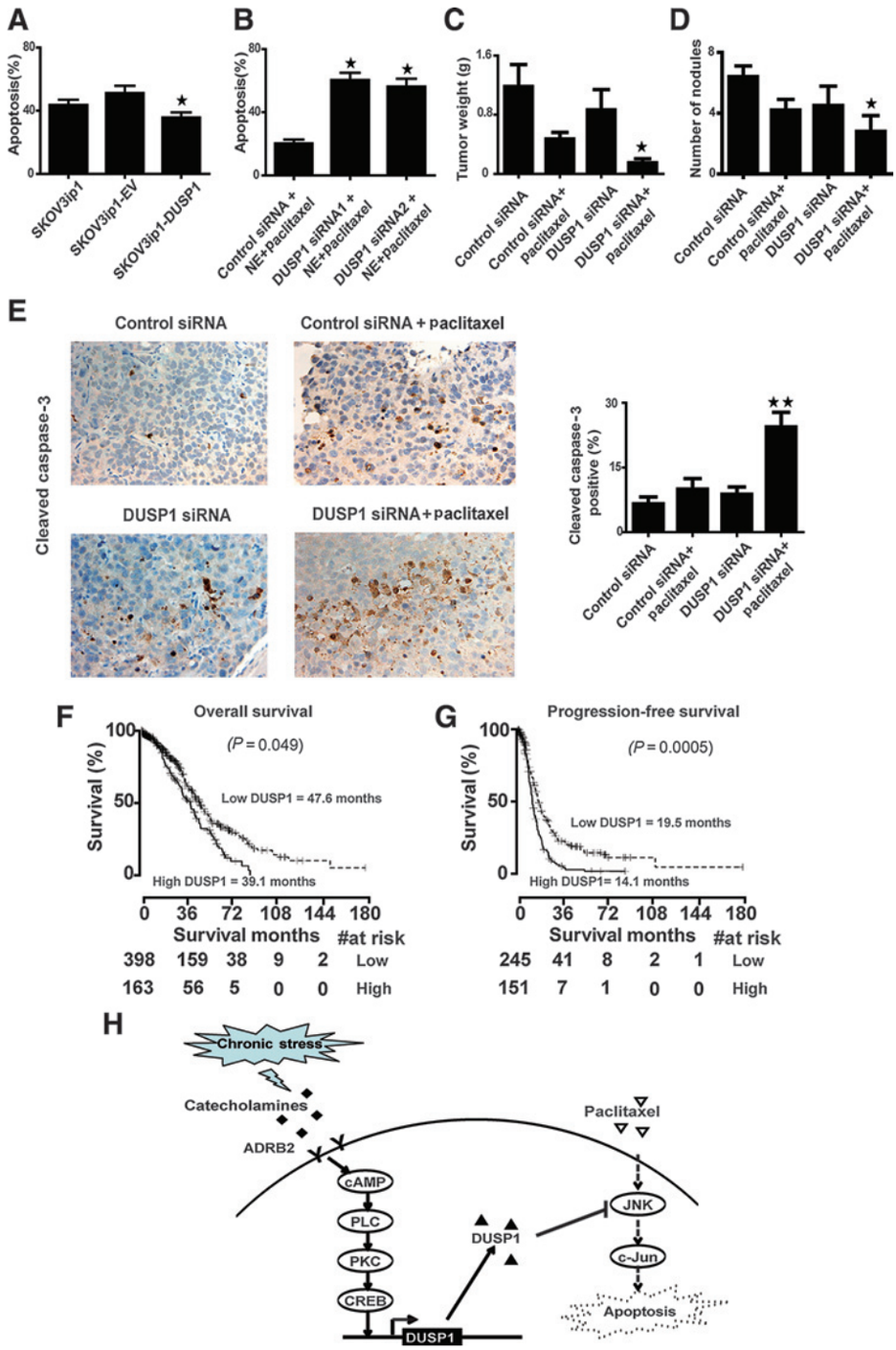

Figure 6.
DUSP1 plays a role in mediating stress-induced chemoresistance. A, analysis of apoptosis in SKOV3ip1 cells overexpressing DUSP1 in no-stress conditions. *, $P < 0.05$, compared with the SKOV3ip1-EV group (cells transfected with pCMV6-entry vector). Error bars, SEM. B, analysis of apoptosis in HeyA8 cells expressing DUSP1 siRNA, treated with norepinephrine (NE) and paclitaxel. *, $P < 0.05$, compared with the control siRNA, norepinephrine, and paclitaxel group. Error bars, SEM. C and D, effects of DUSP1 silencing on stress-mediated tumor growth. Nude mice were subjected to 2 hours of daily restraint stress each morning for 3 to 4 weeks using HeyA8 ovarian cancer models. Mice ($n = 10$ per group) were injected subcutaneously with HeyA8 cells and randomly assigned to 1 of 4 groups: (i) control siRNA twice weekly; (ii) control siRNA twice weekly and intraperitoneal paclitaxel weekly; (iii) DUSP1 siRNA twice weekly; or (iv) DUSP1 siRNA twice weekly and intraperitoneal paclitaxel weekly. After 3 to 4 weeks of treatment, mice were killed and tumor weights and number of nodules were recorded. Mean tumor weight (C) and mean number of nodules (D) are shown in the graphs. *, $P < 0.05$, compared with control siRNA and paclitaxel. Error bars, SEM. E, immunohistochemical analysis of cleaved caspase-3 staining in a sample of tumor tissue from each group. All photographs were taken at 200× magnification. **, $P < 0.01$, compared with control siRNA and paclitaxel. Error bars, SEM. Overall survival (F) and progression-free survival (G): Kaplan–Meier curves for ovarian cancer patients with high and low DUSP1 expression is shown. Median survival durations for each group are shown. Data are compiled from the TCGA project. H, working model of stress-induced chemoresistance. After being exposed to a stressor, catecholamines are released and bind to the β-adrenergic receptors on the tumor cell surface to initiate downstream signaling through cAMP–PLC–PKC and CREB, which initiates transcription of DUSP1 gene expression. DUSP1 protein is produced and JNK and c-Jun are dephosphorylated, protecting the cells from apoptosis.

Functional roles of DUSP1 in response to chemotherapy

Given the role of DUSP1 in apoptosis (12, 13), we further examined its role in protecting cancer cells from apoptosis during exposure to norepinephrine. SKOV3ip1 cells were transiently transfected with a DUSP1-myc/DDK-tagged expression vector; DUSP1 expression increased by about 3-fold in these cells compared with SKOV3ip1 cells transfected with pCMV6-entry vector (Supplementary Fig. S3B). Cells with DUSP1 overexpression showed 43.3% less paclitaxel-induced apoptosis than cells expressing vector alone ($P = 0.018$; Fig. 6A). These data suggest that DUSP1 upregulation contributes to the inhibition of chemotherapy-induced apoptosis. Next, we determined the

effect of DUSP1 siRNA on paclitaxel-induced apoptosis. Forty-eight hours after siRNA transfection, cells were treated with norepinephrine and paclitaxel for 72 hours. As shown in Fig. 6B, DUSP1 siRNA1 expression reversed the norepinephrine-mediated protection from apoptosis. DUSP1 siRNA2 produced similar results (Fig. 6B).

To test the role of DUSP1 *in vivo*, we used the DOPC nanoliposomal delivery method (14, 15). Daily restraint stress resulted in substantially increased DUSP1 levels, whereas treatment with DUSP1 siRNA effectively reduced DUSP1 expression (Supplementary Fig. S3C). To determine the role of DUSP1 in mediating stress-induced tumor growth, female nude mice were injected with HeyA8 cells into the peritoneal cavity and then randomized to one of the following treatment groups ($n = 10$ mice per group): (i) control siRNA twice weekly; (ii) control siRNA twice weekly and intraperitoneal paclitaxel weekly; (iii) DUSP1 siRNA twice weekly; or (iv) DUSP1 siRNA twice weekly and intraperitoneal paclitaxel weekly. Treatment with DUSP1 siRNA significantly improved the efficacy of paclitaxel chemotherapy (Fig. 6C and D). Effects on apoptosis were the highest in the DUSP1 siRNA plus paclitaxel group, which increased apoptosis by 144% compared with the control siRNA plus paclitaxel group ($P = 0.008$; Fig. 6E).

DUSP1 is associated with decreased overall and progression-free survival

Next, we examined for potential correlations between DUSP1 expression and patient outcomes using TCGA. The Cox regression analysis of overall survival yielded a hazard ratio of 1.13 [95% confidence interval (CI), 1.01–1.27; $P = 0.049$) for DUSP1 (201044_x_at; Affymetrix microarray). The Kaplan–Meier plots were generated for the cutoff of 0.71. The Cox regression analysis of disease-free survival yielded a hazard ratio of 1.22 (95% CI, 1.09–1.37; $P = 0.0005$) for DUSP1 (A_32_P171482; Agilent microarray). The Kaplan–Meier plots were generated for the cutoff of 0.62. The data showed high DUSP1 expression was associated with decreased overall survival (Fig. 6F) and decreased progression-free survival (Fig. 6G).

Discussion

The key finding of this study is the discovery of a previously unrecognized pathway by which sustained adrenergic signaling leads to impaired chemotherapy response in ovarian cancer (Fig. 6H). In this model, chronic stress induces the expression of DUSP1 through activation of the ADRB2/cAMP/PLC/PKC/CREB signaling cascade, resulting in JNK-mediated phosphorylation of c-Jun and protection from apoptosis. Our previous work showed that the angiogenic effects of NE/ADRB2 are mediated, in part, via secretion of VEGF (4). Here, we found that VEGF itself has no effects on apoptosis inhibition (Supplementary Fig. S4). Interestingly, it has been reported that HPA mediators, such as glucocorticoids, promote cancer cell survival through DUSP1-dependent pathways (5). However, the role of adrenergic signaling on DUSP1 expression and response to chemotherapy remained unknown until now. These data have particular relevance due to the fact that a substantial proportion of ovarian cancer patients have biobehavioral alterations that would be reflective of chronic stress (16) and are associated with increased catecholamine concentrations in primary tumor tissues (17, 18).

This work provides a rationale for the addition of β-blockers, such as propranolol, to adjuvant therapy to enhance the efficacy of current chemotherapy regimens. β-blockers are commonly used to safely treat hypertension and other cardiovascular maladies. Recent studies have implicated β-blockers in reducing metastatic efficiency and are associated with lower recurrence rates and longer disease-free intervals in several cancers, including ovarian cancer (19–22). Moreover, a phase 0 clinical trial (NCT01308944) is addressing the effects of adding propranolol to first-line chemotherapy for ovarian cancer. Findings from this trial will shed further light on efficacy of β-blockers with traditional chemotherapy for improving the outcome of cancer patients.

In summary, norepinephrine-mediated increase in DUSP1 decreases the antitumor effects of commonly used chemotherapeutic agents. These findings provide a new understanding of how sustained adrenergic signaling leads to impaired chemotherapy response. Our data suggest that interventions targeting the SNS, such as β-blockers, could enhance the efficacy of chemotherapy in patients with ovarian and other cancers.

Disclosure of Potential Conflicts of Interest

No potential conflicts of interest were disclosed.

Authors' Contributions

Conception and design: Y. Kang, R. Rupaimoole, G. Lopez-Berestein, S.W. Cole, A.K. Sood

Development of methodology: Y. Kang, J.M. Hansen, A.K. Sood

Acquisition of data (provided animals, acquired and managed patients, provided facilities, etc.): Y. Kang, G.N. Armaiz-Pena, R. Rupaimoole, R.A. Previs, J.M. Hansen, C. Rodriguez-Aguayo, G. Lopez-Berestein, S.W. Cole, A.K. Sood

Analysis and interpretation of data (e.g., statistical analysis, biostatistics, computational analysis): Y. Kang, W. Hu, R. Rupaimoole, C. Ivan, P. Ram, V. Sehgal, G. Lopez-Berestein, S.W. Cole, A.K. Sood

Writing, review, and/or revision of the manuscript: Y. Kang, A.S. Nagaraja, G.N. Armaiz-Pena, P.L. Dorniak, W. Hu, R.A. Previs, J.M. Hansen, P. Ram, S.K. Lutgendorf, S.W. Cole, A.K. Sood

Administrative, technical, or material support (i.e., reporting or organizing data, constructing databases): W. Hu, K.M. Gharpure, A.K. Sood

Study supervision: A.K. Sood

Acknowledgments

The authors thank Dr. Robert Langley and Donna Reynolds for their assistance with the immunohistochemical analysis. They also thank Erica A. Goodoff in the Department of Scientific Publications for editing this manuscript.

Grant Support

This work was supported by the NIH (CA 109298, P50 CA083639, P50 CA098258, CA140933, and CA104825), the OvarianCancer Research Fund, Inc. (Program Project Development Grant), the Betty Anne Asche Murray Distinguished Professorship and the National Natural Science Foundation of China (grant no. 81472423). J.M. Hansen and R.A. Previs are supported by an NCI–DHHS–NIH T32 Training Grant (T32 CA101642). A.S. Nagaraja is supported by a Research Training Award from the Cancer Prevention and Research Institute of Texas (CPRIT RP140106). K.M. Gharpure is supported by Altman Goldstein Discovery fellowship.

The costs of publication of this article were defrayed in part by the payment of page charges. This article must therefore be hereby marked *advertisement* in accordance with 18 U.S.C. Section 1734 solely to indicate this fact.

Received May 31, 2015; revised October 6, 2015; accepted October 13, 2015; published OnlineFirst November 18, 2015.

References

1. Lutgendorf SK, Sood AK, Antoni MH. Host factors and cancer progression: biobehavioral signaling pathways and interventions. J Clin Oncol 2010;28:4094–9.
2. Su F, Ouyang N, Zhu P, Ouyang N, Jia W, Gong C, et al. Psychological stress induces chemoresistance in breast cancer by upregulating mdr1. Biochem Biophys Res Commun 2005;329:888–97.
3. Flint MS, Kim G, Hood BL, Bateman NW, Stewart NA, Conrads TP. Stress hormones mediate drug resistance to paclitaxel in human breast cancer cells through a CDK-1-dependent pathway. Psychoneuroendocrinology 2009;34:1533–41.
4. Thaker PH, Han LY, Kamat AA, Arevalo JM, Takahashi R, Lu C, et al. Chronic stress promotes tumor growth and angiogenesis in a mouse model of ovarian carcinoma. Nat Med 2006;12:939–44.
5. Wu W, Pew T, Zou M, Pang D, Conzen SD. Glucocorticoid receptor-induced MAPK phosphatase-1 (MPK-1) expression inhibits paclitaxel-associated MAPK activation and contributes to breast cancer cell survival. J Biol Chem 2005;280:4117–24.
6. Sastry KS, Karpova Y, Prokopovich S, Smith AJ, Essau B, Gersappe A, et al. Epinephrine protects cancer cells from apoptosis via activation of cAMP-dependent protein kinase and BAD phosphorylation. J Biol Chem 2007; 282:14094–100.
7. Sun X, Bao J, Nelson KC, Li KC, Kulik G, Zhou X. Systems modeling of anti-apoptotic pathways in prostate cancer: psychological stress triggers a synergism pattern switch in drug combination therapy. PLoS Comput Biol 2013;9:e1003358.
8. Pecot CV, Rupaimoole R, Yang D, Akbani R, Ivan C, Lu C, et al. Tumour angiogenesis regulation by the miR-200 family. Nat Commun 2013; 4:2427.
9. Kang Y, Hu W, Ivan C, Dalton HJ, Miyake T, Pecot CV, et al. Role of focal adhesion kinase in regulating YB-1-mediated paclitaxel resistance in ovarian cancer. J Natl Cancer Inst 2013;105:1485–95.
10. Shahzad MM, Arevalo JM, Armaiz-Pena GN, Lu C, Stone RL, Moreno-Smith M, et al. Stress effects on FosB- and interleukin-8 (IL8)-driven ovarian cancer growth and metastasis. J Biol Chem 2010;285:35462–70.
11. Kristiansen M, Hughes R, Patel P, Jacques TS, Clark AR, Ham J. Mkp1 is a c-Jun target gene that antagonizes JNK-dependent apoptosis in sympathetic neurons. J Neurosci 2010;30:10820–32.
12. Magi-Galluzzi C, Mishra R, Fiorentino M, Montironi R, Yao H, Capodieci P, et al. Mitogen-activated protein kinase phosphatase 1 is overexpressed in prostate cancers and is inversely related to apoptosis. Lab Invest 1997;76:37–51.
13. Castillo SS, Teegarden D. Sphingosine-1-phosphate inhibition of apoptosis requires mitogen-activated protein kinase phosphatase-1 in mouse fibroblast C3H10T 1/2 cells. J Nutr 2003;133:3343–9.
14. Landen CN Jr, Chavez-Reyes A, Bucana C, Schmandt R, Deavers MT, Lopez-Berestein G, et al. Therapeutic EphA2 gene targeting *in vivo* using neutral liposomal small interfering RNA delivery. Cancer Res 2005;65: 6910–8.
15. Pradeep S, Kim SW, Wu SY, Nishimura M, Chaluvally-Raghavan P, Miyake T, et al. Hematogenous metastasis of ovarian cancer: rethinking mode of spread. Cancer Cell 2014;26:77–91.
16. Bodurka-Bevers D, Basen-Engquist K, Carmack CL, Fitzgerald MA, Wolf JK, de Moor C, et al. Depression, anxiety, and quality of life in patients with epithelial ovarian cancer. Gynecol Oncol 2000;78:302–8.
17. Lutgendorf SK, DeGeest K, Dahmoush L, Farley D, Penedo F, Bender D, et al. Social isolation is associated with elevated tumor norepinephrine in ovarian carcinoma patients. Brain Behav Immun 2011;25: 250–5.
18. Lutgendorf SK, DeGeest K, Sung CY, Arevalo JM, Penedo F, Lucci J 3rd, et al. Depression, social support, and beta-adrenergic transcription control in human ovarian cancer. Brain Behav Immun 2009;23:176–83.
19. Stone RL, Nick AM, McNeish IA, Balkwill F, Han HD, Bottsford-Miller J, et al. Paraneoplastic thrombocytosis in ovarian cancer. N Engl J Med 2012;366:610–8.
20. Melhem-Bertrandt A, Chavez-Macgregor M, Lei X, Brown EN, Lee RT, Meric-Bernstam F, et al. Beta-blocker use is associated with improved relapse-free survival in patients with triple-negative breast cancer. J Clin Oncol 2011;29:2645–52.
21. Powe DG, Voss MJ, Zanker KS, Habashy HO, Green AR, Ellis IO, et al. Beta-blocker drug therapy reduces secondary cancer formation in breast cancer and improves cancer specific survival. Oncotarget 2010;1:628–38.
22. Barron TI, Connolly RM, Sharp L, Bennett K, Visvanathan K. Beta blockers and breast cancer mortality: a population-based study. J Clin Oncol 2011;29:2635–44.